Applied Biochemistry and Biotechnology (2022) 194:5037–5059
https://doi.org/10.1007/s12010-022-04017-0

ORIGINAL ARTICLE

Chemical Profiling and In Vitro Antiurolithiatic Activity of *Pleurolobus gangeticus* (L.) J. St.- Hil. ex H. Ohashi & K. Ohashi Along with Its Antioxidant and Antibacterial Properties

Prasobh K. Mohan[1] · T. P. Adarsh Krishna[2] · A. Thirumurugan[1] · T. Senthil Kumar[1] · B. D. Ranjitha Kumari[1]

Accepted: 27 May 2022 / Published online: 10 June 2022

Abstract

Pleurolobus gangeticus (L.) J. St.- Hil. ex H. Ohashi & K. Ohashi (Fabaceae) is an important medicinal plant used to treat various ailments. In this study, we report the antiurolithiatic, antioxidant, and antibacterial potential of chloroform fraction (CF) from *P. gangeticus* roots. For the chemical profiling, HPTLC, FT-IR, and GC–MS techniques of the CF were carried out, and phytochemical investigation was revealed that stigmasterol (45.06%) is one of the major components present in the fraction. The nucleation and aggregation assays were used to evaluate the in vitro antiurolithiatic activity at various concentration (2–10 mg/mL) of the CF. The results showed that the chloroform fraction had dose-dependent effects on Calcium Oxalate (CaOx) crystal formation. In both the assays, the maximum concentration of 10 mg/mL has shown better results. This concentration resulted significant increase in CaOx crystal nucleation along with the reduction of crystal size and the inhibition of crystal aggregation. Further, the CF showed stronger antioxidant (DPPH, NO, SOD, TRC) potential with an IC_{50} values of 415.9327, 391.729, 275.971, and 419.14 µg/mL, respectively. The antibacterial evaluation displayed effective results in the Agar well diffusion assay against selective urinary tract infection (UTI) pathogens (*Escherichia coli*, *Klebsiella pneumonia*, and *Staphylococcus aureus*). A maximum zone of inhibition (ZOI) 12.33 ± 1.05 mm for *K pneumonia* and minimum ZOI of 8.46 ± 0.27 mm for *S. aureus* were obtained. Further, the ADME-PK property of the stigmasterol was investigated, and it was found to pass the Lipinski and Ghose rules, supporting the drug-likeliness. This is the first record of the antiurolithiatic potential of *P. gangeticus* along with antioxidant and antibacterial activities. These findings give an insight into the effective drug development and treatment for kidney stones in future.

Keywords *Pleurolobus gangeticus* · Antiurolithiasis · Antibacterial · Antioxidant · Chemical profiling

✉ Prasobh K. Mohan
prasobhm8@gmail.com

✉ B. D. Ranjitha Kumari
ranjithakumari2004@yahoo.co.in

Extended author information available on the last page of the article

Introduction

Kidney stones are the third most common urinary tract problem with around ten to twelve percent of the population in industrialized countries reporting kidney stones with a high rate of recurrence [1, 2]. Kidney stones patients suffer from severe colic, which cannot be treated with traditional pain killers requiring the use of narcotic analgesics [3]. In addition to pain, obstruction of the urinary tract, urinary tract infections, hydronephrosis, and severe bleeding may occur, and in some cases, surgery may be necessary to remove or break the stones [4]. Kidney stone normally begins as a small crystal-like material, and it gradually builds up into a larger, solid mass. Based on the chemical nature and its composition, commonly occurred urinary stones are referred as calcium oxalate/ phosphate, struvite, uric acid, and ammonium acid [5]. Among these, about 80% of stones are calcium based, and those are calcium oxalate stones [6]. They are usually treated with medications that may cause a number of side-effects. The use of herbs in the prevention and treatment of kidney stone is a useful strategy and safer than synthetic drugs. It has been estimated that 80% of the world's population relies on traditional medicine for treatment [7].

The stone breaking plants are a group of medicinal plants which are used in Indian traditional medicinal system, claimed to be useful in the treatment of kidney stone. Therapeutic effects of medicinal plants on kidney and urinary tract disorders have been studied in various ways, and their effectiveness have been proven [8]. In recent years, the antiurolithiatic potential of several extracts from different parts of various medicinal plants such as *Prunus cerasoides* [9], *Boldoa purpurascens* [10], *Micromeria fruticosa* [11], and *Pleroma pereirae* [12] has been reported. The use of such extracts may lead to the complementary and alternative medicine against synthetic drugs. In this scenario, this study aims to elucidate the antiurolithiatic ability of *Pleurolobus gangeticus* (L.) J. St.- Hil. ex H. Ohashi & K. Ohashi root along with its antioxidant and antibacterial properties.

This plant species, formerly *Desmodium gangeticum* (L.) DC, has emerged as a vital ingredient of traditional medicine, and it belongs to the Fabaceae family [13]. In Ayurvedic System of Medicine (ASM), the various parts of this species are used as febrifuge, bitter tonic, digestive medicine, anti-catarrhal, and antiemetic, in inflammatory conditions of the chest and in various other inflammatory conditions [14, 15]. Many of the Ayurvedic formulations such as "Dashmoola Kwatha" and "Dashamoolarishta" contain this medicinal plant, and it is often known by the moniker "Master of medicinal plants" [14, 16]. The plant is known to be a rich source of important phyto-constituents such as flavonoids, alkaloids, sterols, glycolipids, terpenoids, pterocarpans and coumarins [17]. In addition, elements such as calcium (Ca), phosphorus (P), and magnesium (Mg) were reported from the plant. This chemical variety has made this species highly medicinal, and the plant has been reported for its antidiabetic [18] antiamnesic [19], antibacterial [20], antiinflammatory [21], antinociceptive [22], antioxidant [23], cardioprotective [24], hepatoprotective [25] and antileishmanial [26] properties. Till date, there has been no report on the antiurolithiatic properties of this plant species to our knowledge. This preliminary investigation may help the identification of a new antiurolithiatic agent from this plant species.

Materials and Methods

Collection and Identification of Plant Sample

Pleurolobus gangeticus (L.) J. St.- Hil. ex H. Ohashi & K. Ohashi (Fabaceae) was collected from the Idukki (Latitude, 10.0891° N/Longitude, 77.0597° E) District of Kerala,

India. The plant was identified from Botanical Survey of India (Southern Region Center) Voucher Number: BSI/SRC/5/23/2021/Tech/156.

Preparation of Chloroform Fraction (CF)

Fresh roots of *P. gangeticus* were collected and washed thoroughly with water and dried in shade. One hundred grams of air-dried roots was ground to fine powder and soaked in 80% aqueous ethanol for 48 h with continuous stirring. After soaking, the mixture was then filtered with Whatman No. 1 filter paper. The filtrate obtained was centrifuged at 10,000 rpm at room temperature (25 °C), and the pellet was discarded. The supernatant was collected and concentrated *in vacuo* by means of rotavapor.The concentrated extract was then washed with *n*-hexane; further, it was suspended in distilled water and fractionated with chloroform in a stepwise manner [27].

High-Performance Thin Layer Chromatography (HPTLC) Profiling

High-performance thin layer chromatography (HPTLC) analysis was carried out on a HPTLC (Camag, Switzerland) system with chloroform fraction of *P. gangeticus*. TLC plates precoated with silica gel 60 F254 (20 × 10 cm with 200-µm layer thicknesses) from Merck, Germany, were used for the chromatographic separation of the sample. Five microliter of CF (2 mg/mL) was spotted onto the plates with 8 mm bandwidth using Camag 100 µL sample syringe (Hamilton, Switzerland) and Camag Linomat 5 applicator (Camag, Switzerland). Linear ascending development was carried out in a twin trough glass chamber with Hexane:Ethyl acetate (8:2). Scanning was performed using Camag TLC scanner 3 at 254 nm and 366 nm through fluorescence mode and operated by win CATS software (version 1.4.1, Camag). Plates were visualized under UV 254 nm, UV 366 nm and in visible light.

Fourier Transform Infrared (FTIR) Profiling

The spectra used in obtaining the structural properties of the chloroform fraction of *P. gangeticus* were obtained from the FTIR spectrometer equipped with an attenuated total reflectance (ATR-FTIR), model Perkin-Elmer Spectrum 400. In the ATR-FTIR method, the sample to be analyzed is placed directly into the sample cell, where a good and reproducible contact between the sample and the crystal of reflection is obtained non-destructively, producing good quality infrared spectra. The FTIR spectra were recorded in the range of 4,000,700 cm^{-1}.

Gas Chromatography-Mass Spectrometry (GC–MS) Profiling

The identification of chemical constituents present in the CF of *P. gangeticus* was determined by GC–MS (Agilent 7250 GC/Q-TOF). The high-resolution GC/Q-TOF enables accurate mass screening by GC/MS and enhanced compound identification through MS/MS (Detector: Microchannel plate/scintillator/PMT; ADC electronics), equipped with

low-energy electron ionization and complimentary chemical ionization techniques at an initial column temperature of 30 °C heated up to 300 °C at 10 °C per 4 min. Helium was used as the carrier gas. Exactly 1 μL of the sample was injected with splitless mode. The ionization voltage was 70 eV. MS scan range was set at 45–450 (MHz). The total running time for a sample was 55 min. The chemical constituents were identified by GC–MS. The compounds fragmentation patterns of mass spectra were compared with those stored in the spectrometer database from the National Institute of Standards and Technology (NIST) Mass Spectral Library.

Pharmacokinetics and Drug-Likeness Profiling

Pharmacokinetics and drug-likeness prediction for the compound stigmasterol (identified from CF through GC/MS profiling) was performed by online tool Swiss-ADME [28] of the Swiss Institute of Bioinformatics (http://www.sib.swiss) [29]. 2D structural models were drawn in ChemBioDraw Ultra version 15.0 (Cambridge Software), and SMILES of stigmasterol was translated into molfile by online SMILES translator and structure file generator found in online tool Swiss-ADME. The analysis task was done to check whether the compound was an inhibitor of isoforms of the Cytochrome P450 (CYP) family, such as CYP1A2, CYP2C19, CYP2C9, CYP2D6, and CYP3A4. Also, pharmacokinetics (such as gastrointestinal absorption, P-glycoprotein, and blood–brain barrier) and drug-likeness prediction such as Lipinski and Ghose rules and bioavailability score were done [30–32]. The Lipinski and Ghose rules were applied to assess drug-likeness to predict whether a compound was likely to be bioactive as per important parameters such as molecular weight, Log P, number of HPA, and HBD. The Swiss-ADME tool used a vector machine algorithm (SVM) [33] with fastidiously cleaned large datasets of known inhibitors/non-inhibitors as well as substrates/non-substrates.

Antiurolithiatic Assay

(a) Nucleation Assay

Calcium chloride ($CaCl_2$) and sodium oxalate ($Na_2C_2O_4$) solutions were prepared separately, at final concentrations of 5 and 7.5 mmol/L, respectively, in a buffer (0.05 mol/L Tris-HCl and 0.15 mol/L NaCl) at pH 6.5; both solutions were filtered with a Millipore filter paper. For the assay, 950 μL of calcium chloride and 100 μL of CF (2, 4, 6, 8, and 10 mg/mL) were mixed. To this mixture, 950 μL of sodium oxalate was added and stirred well. Afterwards, it was incubated at 37 °C for 30 min. The absorbance was measured at 620 nm with an ultraviolet (UV) visible spectrophotometer (Jasco, UV/VIS Spectrophotometer). Reaction mixture was prepared without the extract was considered as the blank. Experiments with each test sample were carried out in triplicates. Morphology and number of the CaOx crystals formed were also observed using a Leica DM 2500 LED microscope [34, 35].

(b) Aggregation Assay

Solutions of calcium chloride and sodium oxalate at 50 mmol/L were prepared with distilled water and mixed well to form the calcium oxalate (CaOx) crystals. The mixture was then heated to 60 °C on a water bath for 1 h and then allowed to cool at 37 °C overnight.

The mixture was then centrifuged at 2500 rpm for 10 min, and the supernatant decanted and the pellets were collected to get the CaOx crystals. A 1 mg/mL solution of CaOx crystals was prepared in Tris–HCl (0.05 mol/L) and NaCl (0.15 mol/L) buffer at pH 6.5. About 100 µL of CF (2, 4, 6, 8, and 10 mg/mL) was added to the buffered solution of CaOx crystals and was mixed properly and the absorbance read at 620 nm wavelength. Experiment with each test sample was carried out in triplicates [36, 37].

Antioxidant Assay

(a) DPPH Radical Scavenging Assay

The free radical scavenging activity of CF of *P. gangeticus* roots was determined by using DPPH method [38]. Briefly, 0.1 mM solution of DPPH was prepared in 95% methanol and 1 mL of this solution was added to 3.0 mL of CF of *P. gangeticus* roots at different concentrations (100, 200, 300, 400, and 500 µg/mL). Ascorbic acid was used as the standard for the assay. The reaction mixtures were incubated for 30 min under dark condition at room temperature. Then the absorbance was measured at 517 nm, and the IC_{50} values were calculated. The experiment was carried out in triplicate, and the DPPH scavenging potential was evaluated.

(b) NO Radical Scavenging Assay

One hundred microliter of CF and standard ascorbic acid at 100–500 µg/mL concentration were added separately to 1 mL of 10 mM phosphate buffered saline at pH 7.4 containing 10 mM sodium nitroprusside and mixed well. This reaction mixture was kept under incubation for 2 h at 30 °C. After incubation, 500 µL of Griess reagent (1% sulfanilamide, 2% H_3P0_4, and 0.1% N-(1- naphthyl) ethylenediamine dihydrochloride) was added. Then the absorbance was read at 550 nm. [39].

(c) Superoxide Radical Scavenging Assay

Nitro Blue Tetrazolium (NBT) solutions (156 mM NBT in 100 mM phosphate buffer, pH 8.0) were prepared, and 1 mL of it is mixed with 1 mL of nicotinamide adenine dinucleotide (NADH) solution (468 mM in 100 mM phosphate buffer, pH 8.0). To this mixture, 100 µL of 100 to 500 µg/mL of CF and standard ascorbic acid was added separately. To the above reaction mixture, 100 µL phenanzine methosulfate (PMS) solution (60 mM PMS in 100 mM phosphate buffer, pH 8.0) was added and incubated at 25 °C for 5 min. After incubation, the absorbance was measured at 560 nm [40].

(d) Total Reduction Capability

The total reducing capacity of the CF was determined according to the method adopted by [41]. Briefly, 2.5 mL of 0.2 M phosphate buffer at pH 6.6 containing (1% w/v) potassium ferricyanide ($K_3Fe(CN)_6$) was added separately to 100 µL of different concentrations (100–500 µg/mL) of CF and standard ascorbic acid. This reaction mixture was incubated at 50 °C for 20 min. After incubation, 2.5 mL of (10% w/v) trichloroacetic acid (TCA) was added to each tube, and the reaction mixture was centrifuged at 3000 rpm for 10 min, and the supernatant was collected. 2.5 mL of the supernatant was mixed with 2.5 mL of

distilled water, and 0.5 mL of $FeCl_3$ (0.1%, w/v) solution was added, and the absorbance was read at 700 nm.

Antibacterial Assay

(a) Test Pathogens

Pure bacterial cultures of *Escherichia coli* (MTCC-1687), *Klebsiella pneumonia* (MTCC-3384), and *Staphylococcus aureus* (MTCC-3163) were obtained from Microbial Type Culture Collection (MTCC).

(b) Agar Well Diffusion Method

The antibacterial activity of CF of *P. gangeticus* against selected UTI pathogens was evaluated by agar well diffusion method [42]. The overnight inoculated bacterial cultures were spread over freshly prepared Muller-Hinton agar plates using sterile cotton swabs. Wells of 6 mm in size were prepared using a sterile cork borer (HiMedia), and the wells were loaded with diluted sample (100 µL of 10 mg/mL concentration) of CF. Ampicillin (15 µg) were used as the positive control for the study. All the plates were incubated at 37 °C for 24 h. After the completion of incubation period, the zones of inhibition (ZOI) (mm) were measured and noted.

Statistical Analysis

The results were expressed as Mean ± SD. All the values were statistically evaluated using SPSS version 16.0 by means of one-way analysis of variance (ANOVA) followed by Duncan's multiple range test (DMRT). Mean values were considered statistically significant when $p < 0.05$.

Results and Discussion

Plants contain a diverse range of bioactive compounds having definite applications, especially in the fields of medicine [43]. Pharmacologically active compounds are identified from plants mostly through biological activity guided extraction and isolation from crude drugs leading to the discovery of many new drug candidates. Moreover, the use of herbal medicine has many advantages over synthetic drugs including being inexpensive and eco-friendly.

The chemical profile of a crude drug depends on its genetic constitution, geographical location, growth conditions, soil chemistry, and season of harvest of the plant [44]. Extraction is the main process by which bioactive molecules can be obtained from biomass, and the main objective of extraction technique is to maximize the amount of target molecules and to obtain the highest chemical biology of these extracts [45]. The extraction yield and chemical biology of the resultant extract is not only affected by extraction techniques like microwaves, ultrasonic, pressurized liquids, supercritical fluids, and electric fields [46] but also by the extraction solvent [47]. Scientists have reported the impact of different type of solvents on bio-molecule extraction [48, 49]. Generally, polar (ethyl acetate, chloroform,

acetone, ethanol, methanol, and water) and non-polar (hexane, benzene, and petroleum ether) solvents are used for extracting bioactive compounds from plant materials [50]. Chloroform extract or fraction derived from *P. gangeticus* has various pharmacological activities, including antiamnesic [51], inotropic [52], antileishmanial and immunomodulatory [53], antiinflammatory [54], and psychopharmacological [55] activities.

This study was conducted to elucidate the antiurolithiatic ability of the chloroform fraction (CF) of *P. gangeticus* root against calcium oxalate (CaOx) crystals as part of our pursuit of new and safe antiurolithiatic agents. Moreover, we have also attempted to evaluate the antioxidant and antibacterial potential of CF to establish a possible mechanism for the same. For CF, air-dried roots were pulverized using a milling machine and extracted with 80% aqueous ethanol by using a shaker for 48 h at room temperature (RT). The extract was filtered and concentrated, washed with *n*-hexane, and was subsequently suspended in distilled water and fractionated with chloroform in a stepwise manner, resulting in a brownish gummy CF with 6.2% yield. Its preliminary phytochemical profiling indicated the presence of amino acids, phenols, alkaloids, flavonoids, coumarins and triterpenoids (Table 1). Many previous phyto-chemical studies on CF of various plant materials were in agreement with the present findings and supported it [56–58].

High-performance thin layer chromatography (HPTLC) is appropriate for the expansion of chromatographic fingerprints to determine major active phyto-constituents through phytochemical marker profiling [59]. The separation and resolution are much better, and the results are much more reliable and reproducible than TLC [60]. It is integrated with digital scanning profiling, densitometry scanning being the main advantage of in situ qualitative and quantitative measurements. Also, a colorful pictorial HPTLC image provides additional and intuitive visual color and/or fluorescence parameters for parallel evaluation of the same TLC plate. It also provided better differentiation of individual/single secondary metabolites [59]. Extracts from various medicinal/aromatic plants have been reported through HPTLC profiling in the past [61, 62]. The present study on HPTLC profiling of CF indicates the occurrence of at least 14 different polyvalent components (Fig. 1). The developed chromatogram will be specific with selected solvent system as hexane: ethyl acetate (8:2) and scanned at 254 nm. The peaks with R_f values of 0.02 (11.10%), 0.15 (10.75%), 0.21 (11.88%), and 0.54 (16.61%) were found to be more prominent. The remaining components are less in quantity; the percentage area of all peaks ranges between 0.96 and 8.99%. The details of major peak are

Table 1 Preliminary phytochemical profiling of CF of *P. gangeticus*

Phytochemical compounds	Inferences
Amino acid	+
Phenols	+
Alkaloids	+
Flavonoids	+
Coumarins	-
Phytosterols	+
Triterpenoids	+
Saponins	-
Volatile oils	-

(+), present; (−), absent

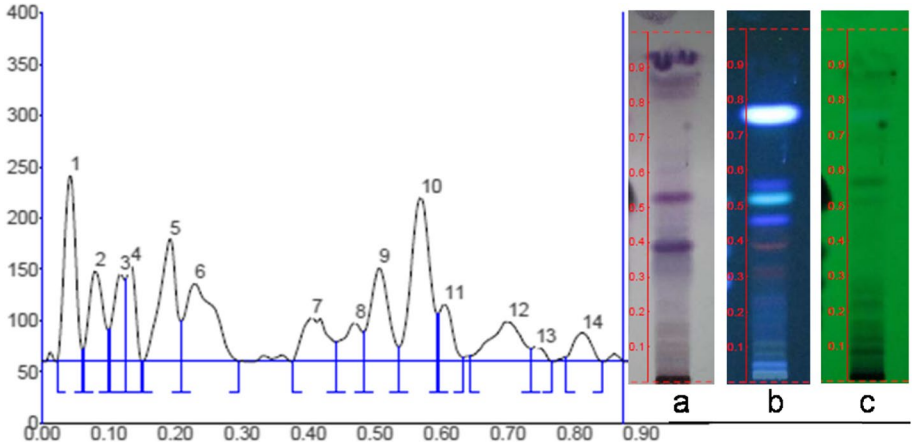

Fig. 1 HPTLC profiling of CF of *P. gangeticus.* **a** TLC plate visualized at visible light, **b** TLC plate visualized at 366 nm, **c** TLC plate visualized at 254 nm

described in Table 2. These sets of information are helpful for the further isolation of individual components from this fraction.

FTIR offers a rapid and non-destructive investigation into fingerprint of plant extracts. In general, the phyto-extracts contains various classes of compounds which have different bonds (C–C, C = C, C ≡ C, C–O, C = O, O–H and N–H). These kinds of bonds can be identified by detecting the characteristic frequency absorption band in the infrared spectrum [63, 64]. In the present study, the functional group (FG) identification was made by FTIR profiling, and seven characteristic peaks were found (Fig. 2). The strong intense peaks are observed at 2924.18 cm^{-1} (range 2935–2915 cm^{-1}) assigned to the H-bonded/O–H stretching vibration, and it indicated the presence of hydroxyl/alcohol/phenolic compounds in the fraction. The peak at 2853.96 cm^{-1} implied a symmetric stretching of –CH-(CH_2)- vibrations corresponding to fatty acids/lipids/protein. Moreover, characteristic peak at 1711.50 cm^{-1} (range 2100–1800 cm^{-1}) and 1464.92 cm^{-1} (range 1510–1450 cm^{-1}) was assigned to the carbonyl compound and aromatic ring vibration, demonstrating the existence of some carbonyl and aromatic compounds in the chloroform fraction.

Table 2 HPTLC major peak details of CF of *P. gangeticus*

Peak	Start R_f	Start height	Max R_f	Max height	Max %	End R_f	End height	Area (AU)	Area %
1	0.02	0.9	0.04	182.3	16.30	0.06	11.0	2828.3	11.10
2	0.06	12.4	0.08	88.5	7.91	0.10	30.7	1734.5	6.81
5	0.15	0.6	0.19	120.0	10.73	0.21	39.3	2738.2	10.75
6	0.21	39.5	0.23	76.3	6.82	0.29	0.2	3026.4	11.88
9	0.48	29.1	0.51	91.5	8.18	0.54	14.4	2290.0	8.99
10	0.54	14.6	0.57	160.2	14.33	0.59	46.1	4230.5	16.61
12	0.65	5.7	0.70	38.9	3.48	0.73	12.9	1690.5	6.64

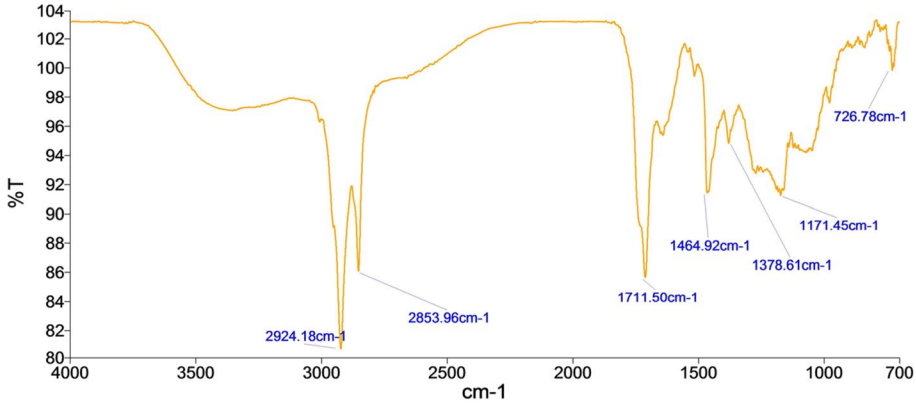

Fig. 2 FTIR spectra of CF of *P. gangeticus*

The results of the GC–MS analysis of the CF revealed the presence of 25 compounds based on the separation of the individual peaks by the GC (Fig. 3). The mass spectra of these compounds were matched with the spectra of known compounds listed in NIST spectral databases and the main components of which are illustrated in Table 3. The major component in the CF of *P. gangeticus* was identified as stigmasterol with 45.06% followed by 14-methyl palmitic acid (7.28%), octyl phthalate (5.17%), palmitic acid (5.14%), and 2,4-di-tert-butylphenol (5.12%).

Stigmasterol, also known as stigmasterin, is an unsaturated phytosterol present in various medicinal plants. In the present chemical investigation, stigmasterol was found to be a major component of the CF of *P. gangeticus*. Stigmasterol is involved in the synthesis of many hormones like androgens, estrogens, corticoids, and progesterone. Moreover, this molecule is already reported for several biological activities such as larvicidal activity [65], antimicrobial [66], antiinflammatory [67], and antioxidant [68]. In addition to stigmasterol, many of its derivatives like stigmasterol glucoside,

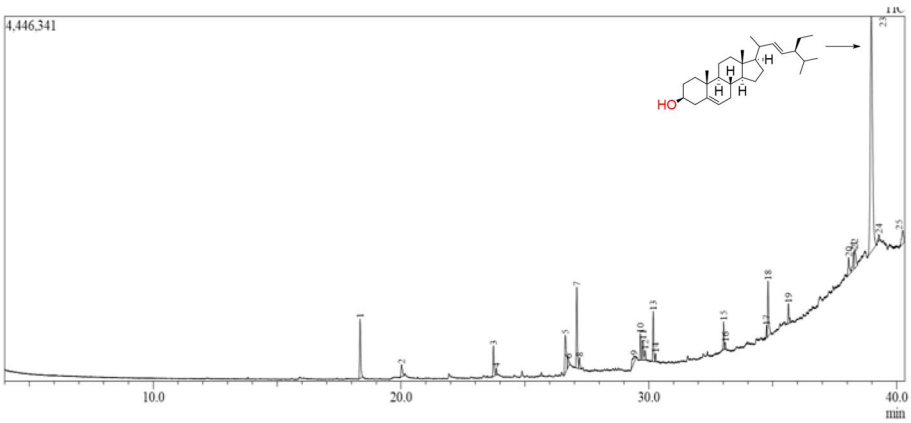

Fig. 3 Chromatogram for the GC–MS profile of *P. gangeticus*

Table 3 GC–MS profiling of CF of *P. gangeticus*

Sl. no	Retention time	Peak no	Name	Molecular formula	Area %
1	18.346	1	2,4-Di-tert-butylphenol	$C_{14}H_{22}O$	5.12
2	20.024	2	1-Pentadecene	$C_{15}H_{30}$	1.42
3	23.731	3	1-Nonadecene	$C_{19}H_{38}$	2.68
4	26.627	5	Palmitic acid	$C_{16}H_{32}O_2$	5.14
5	27.095	7	14-Methyl palmitic acid	$C_{19}H_{38}O_2$	7.28
6	29.401	9	Tridecanediol	$C_{13}H_{24}O_2$	1.84
7	29.663	10	Linoleic acid ethyl ester	$C_{20}H_{36}O_2$	2.01
8	29.759	11	Ethyl oleate	$C_{20}H_{38}O_2$	1.71
9	30.18	13	Lignocerol	$C_{24}H_{50}O$	4.16
10	33.016	15	Heptacosanol	$C_{27}H_{56}O$	2.03
11	34.809	18	Octyl phthalate	$C_{24}H_{38}O_4$	5.17
12	35.633	19	1-Heptacosanol	$C_{27}H_{56}O$	1.60
13	38.063	20	1-Eicosanol	$C_{20}H_{42}O$	1.86
14	38.978	23	Stigmasterol	$C_{29}H_{48}O$	45.06
15	40.247	25	23-Dehydro-beta-sitosterol	$C_{29}H_{48}O$	2.27

fucosterol, fluorostigmasterol, cyasterone, spinasterol, and fucosterol epoxide have also demonstrated potent pharmacological properties [69].

In this context, we tried to understand the pharmacokinetics and drug-likeness properties of stigmasterol through an in silico study. The computer modeling of ADME-PK properties of compounds provides an idea about structure–property relationships and drug metabolism and pharmacokinetics properties based on its chemical structure [70]. We recently successfully demonstrated the pharmacokinetics and drug-likeness properties of pterocarpans [44], quinones [71], and phenothiazines [72]. In silico approaches are applied at an early phase of the drug development process, in order to remove molecules with poor ADME-PK properties and making significant savings in research and development costs.

The chemical structure and physicochemical properties (Lipinski's rule) of stigmasterol were analyzed as per our previous study [73], and the same is illustrated in Table 4. These information help to determine whether a biologically active chemical is having the physico-chemical properties to be orally bioavailable. The ADME-PK studies of stigmasterol revealed low gastrointestinal (GI) absorption and lack blood–brain barrier (BBB) permeability and P-glycoprotein (P-gp) permeability (Table 5). Moreover, the lipophilicity (log $P_{o/w}$) and skin permeation (log Kp) of stigmasterol was found to be 6.97 and − 2.74, respectively. Furthermore, the compound showed inhibition of CYP2C19 (cytochrome P450 isomer). The topological polar surface area (TPSA) was 20.23 Å (≤ 140 Å), indicating that compounds have appropriate oral bioavailability (0.55). The compound meets the criteria of drug-likeness assessment based on Lipinski and Ghose rule (Table 6).

Urine is supersaturated in calcium oxalate (CaOx) implying that it will contain CaOx crystalline particles that are formed spontaneously. Nucleation is an initial step in this where the supersaturated solution is converted to solid phase [74].When crystalline particles are retained within the kidney, they can grow to become full-size stones through growth and aggregation processes. Our in vitro inhibitory effect of CF on CaOx crystallization begins with nucleation assay. For this, different concentrations (2, 4, 6, 8, and 10 mg/mL) of test solution of CF were prepared, and the inhibitory effect was tested and depicted in Table 7.

Table 4 Chemical structure and physicochemical properties of stigmasterol identified from the CF of *P. gangeticus*

No.	Properties	Stigmasterol
1.	2D structure	: 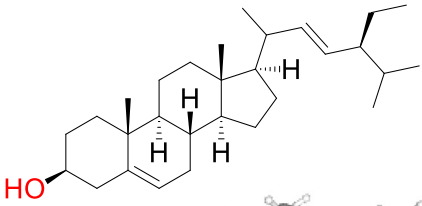
2.	3D structure	: 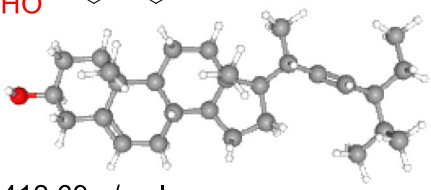
3.	Molecular mass	: 412.69 g/mol
4.	Molecular formula	: $C_{29}H_{48}O$
5.	Molecule class	: Sterol
6.	H-bond acceptor	: 1
7.	H-bond donor	: 1
8.	Rotatable bond	: 5
9.	Heavy atoms	: 30
10.	Molar Refractivity	: 132.75
11.	TPSA	: 20.23 Å²

Table 5 Pharmacokinetic studies of stigmasterol identified from the CF of *P. gangeticus*

Pharmacokinetics properties									
GI absorption	BBB permeation	Log $p_{o/w}$	P-*gp*	Inhibition of Cytochrome P450					Log *Kp*
				CYP1A2	CYP2C19	CYP2C9	CYP3A4	CYP2D6	
Law	No	6.97	No	×	×	√	×	×	-2.74 cm/s

GI, gastrointestinal absorption; *BBB*, blood–brain barrier permeability; *Log P* $_{o/}$*w*, lipophilicity; *P-gp*-, P-glycoprotein substrate; Log *Kp*, Skin permeation

The minimal turbidity at 2 mg/mL of the extract was observed to be 0.377 ± 0.006, and the maximum absorbance at 10 mg/mL was observed to be 0.652 ± 0.006. In control, the addition of sodium oxalate solution into $CaCl_2$ solution results in the formation of numerous large CaOx crystalline particles (Fig. 4A). Similarly, the presence of CF leads to an increase in turbidity with the formation of small fine crystals (Fig. 4B–F). When compared

Table 6 Drug-likeness and medicinal chemistry of stigmasterol identified from the CF of *P. gangeticus*

Drug-likeness and medicinal chemistry										
Log *s*	Drug-likeness					Bio-availability	Medicinal properties			Synthetic accessibility
	Lipinski	Ghose	Veber	Egan	Mugge		TPSA (A^2)	PAINS (alert)	Lead likeness	
−5.47	√	×	√	×	×	0.55	20.23	0	No*	6.21

Log s, solubility class; *TPSA*, topological polar surface area; PAINS, pan assay interference structure; *Molecular weight < 350 and XLOGP3 > 3.5

Table 7 Effects of CF of *P. gangeticus* on CaOx crystal nucleation

Group	Concentration (mg/mL)	Optical density at 620 nm
Control		0.314 ± 0.019^{f}
	2	0.377 ± 0.006^{e}
	4	0.412 ± 0.014^{d}
CF	6	0.499 ± 0.007^{c}
	8	0.590 ± 0.002^{b}
	10	0.652 ± 0.006^{a}

Values are mean of triplicate determination ($n = 3$) ± standard deviation; means bearing different superscripts (a/b/c/d/e/f) indicates significant difference when compare with control; $p < 0.05$; *CF* chloroform fraction

to the control, the absorbance was observed to be more with increased concentration of CF (Table 7). Results of our microscopic evaluation corroborate the findings of the assay. It showed a gradual increase in the number of crystals with reduced size in the presence of the CF (Fig. 5). Stones with smaller size have the possibility of spontaneous passage and elimination through the urinary tract without any discomfort [75, 76]. These results showed a promising outcome for the study. Bawari and co-workers reported antiurolithiatic potential of wild Himalayan cherry (*Prunus cerasoides*) through CaOx crystal. In this assay, they found turbidity and formation of small fine crystalline particles depend up on the concentration of test solution [9]. Likewise, similar observations also found in *Desmodium styracifolium* [77] and *Betula alba* [78].

The microscopic evaluation showed a morphological conversion of calcium oxalate monohydrate (COM) crystals to calcium oxalate dihydrate (COD) crystals in the test

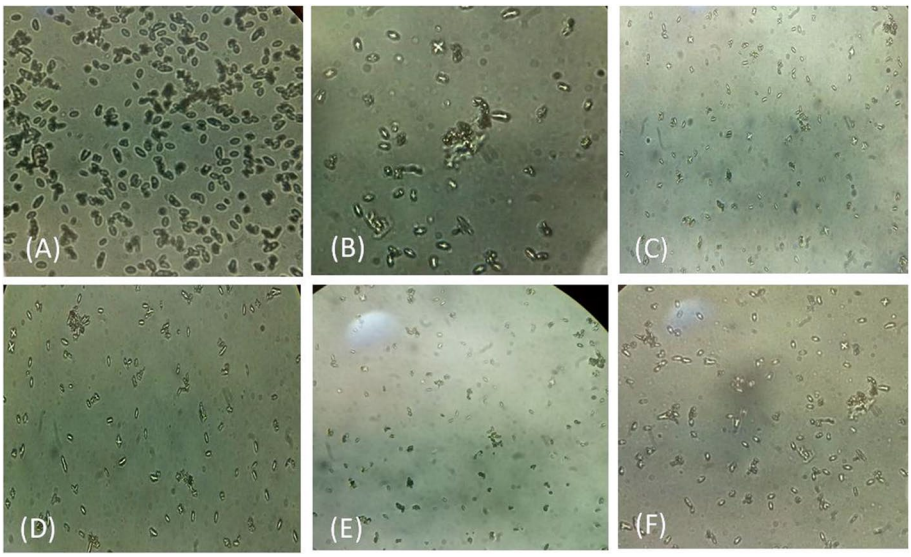

Fig. 4 Representative photographs of CaOx crystals from in vitro crystallization experiment as observed under light microscope (×40). **A** Control, **B** 2 mg/mL, **C** 4 mg/mL, **D** 6 mg/mL, **E** 8 mg/mL, **F** 10 mg/mL

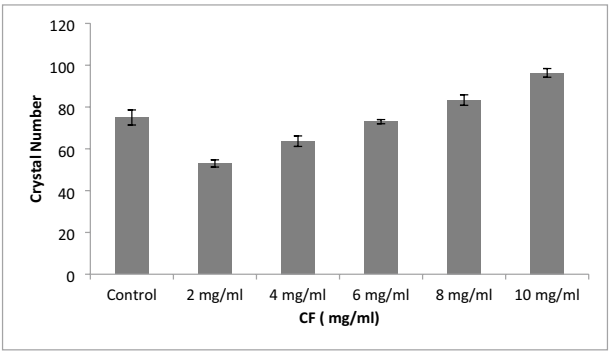

Fig. 5 Number of crystals observed in the CaOx crystallization assay

solution. The transformation of pointy edged dendritic COM crystals to octahedral shaped COD crystals with reduced size and number through the inhibition of COM crystals showed in Fig. 4. This clearly indicates the COM crystal inhibitory potential of the CF. The COM crystals are thermodynamically more stable and bound tightly to the renal epithelial cell surface than the COD crystals, and this will cause renal tubular damage and form difficulties [79]. Moreover, COM crystals show more affinity and strong attachment to the renal epithelial cells than the COD crystals, and this leads to the retention of stones in the kidney [80].So, the transformation from COM to COD is considered as an important step in the treatment of urolithiasis. Similar findings are reported in various plant extracts [80–82]. For example, hydro-alcoholic extract from the *Bergenia ciliate* significantly inhibited the formation and reduction of size of the COM crystals, and meanwhile, it promotes the COD crystals with reduced size [81].

Aggregation is considered as a crucial and final step in urolithiasis, and it is the key factor behind stone retention. During the process, stones get aggregated within a short time, and its elimination through urethra is obstructed [83]. Our results showed gradual increase in absorbance in a dose-dependent manner at all concentrations (Table 8). The turbidity was found to be 0.349 ± 0.007 at 2 mg/mL concentration of CF, whereas the absorbance was found to be increasing to 0.761 ± 0.005 at 10 mg /mL concentration. Absorbance

Table 8 Effects of CF of *P. gangeticus* on CaOx crystal Aggregation

Group	Concentration (mg/mL)	Optical density at 620 nm
Control	-	0.315 ± 0.039^{f}
	2	0.349 ± 0.007^{e}
	4	0.452 ± 0.032^{d}
CF	6	0.572 ± 0.013^{c}
	8	0.679 ± 0.007^{b}
	10	0.761 ± 0.005^{a}

Values are mean of triplicate determination ($n = 3$) ± standard deviation; means bearing different superscripts (a/b/c/d/e/f) indicates significant difference when compare with control; $p < 0.05$; *CF* chloroform fraction

increases due to the breakdown of preformed calcium oxalate crystals into fine particles in the solution. The CF also allows the CaOx crystals get dispersed in the solution and this will help its elimination during the urination and reducing the severity and retention of the stones. The results showed clear inhibitory action against the agglomeration of crystals. Similar findings were previously recorded by several authors and found the clear inhibition of the aggregation of crystals by various plant extracts. Recent reports on the antiurolithiatic potential of betulin obtained from *Betula alba* found to be efficient in preventing the crystal aggregation, and the results showed significant increase in turbidity along with the increase in concentration of the extract [78]. The aqueous extract obtained from *Phyllanthus niruri* found to be effective in preventing the CaOx aggregation and is capable of interfering with the early stages of stone formation [84]. Similar results also observed in the extract of *Eysenhardtia polystachya* [85]. All these findings supported the outcome of the present study.

The oxalate triggered damages occurring in the renal epithelial cells may also be a reason for urolithiasis [78]. The exposure of renal epithelial cells to different type of crystals like CaOx, calcium phosphate, and uric acid produces reactive oxygen species (ROS) [86]. The production of reactive oxygen species (ROS) is also found to be a reason for the development of kidney stones, and it causes damages to the renal epithelial cells through the collapse of oxidant–antioxidant balance in the kidney [87]. The crystal attachment to the tubular cells causes oxidative stress, and it leads to the renal cell injury [88]. The membrane damage also occurs as a result of the absence or reduction of antioxidant enzymes [89]. Thus, the antioxidants have the capacity to prevent the ROS production and to protect the renal epithelial cells from further damage. Plant secondary metabolites are well known for their potential to ameliorate ROS-mediated oxidative stress, which could be beneficial in the management of urolithiasis [88].

In the DPPH assay, the CF of *P. gangeticus* showed strong inhibition of DPPH radical when compared to the standard ascorbic acid. The fractions showed the capacity to reduce the stable DPPH radical (purple) to its non-radical form DPPH (yellow). Maximum percentage of inhibition of 71.33% was observed at 500 µg/mL, and minimum percentage of inhibition of 37.66% was observed at 100 µg/mL. The half maximal inhibitory concentration (IC_{50}) is 415.9327 µg/mL. The DPPH scavenging potential of CF is depicted in Table 9.

The CF of *P. gangeticus* showed strong promising reduction of the nitrite levels formed due to the decomposition of nitroprusside. Maximum percentage of inhibition of 52.66% at 500 µg/mL concentration and minimum percentage of inhibition of 18.33% at 100 µg/mL concentration were estimated. The half maximal inhibitory concentration (IC_{50}) was 391.729 µg/mL. The NO radical scavenging potential of CF is depicted in Table 9.

In the superoxide radical–scavenging assay, the generated super oxide anion radicals react with NBT and form coloration, measured at 560 nm. The results observed are depicted in Table 9. Maximum percentage of inhibition of 56.66% at 500 µg/mL concentration and minimum percentage of inhibition of 14.66% at 100 µg/mL concentration were observed. The half maximal inhibitory concentration (IC_{50}) was 275.971 µg/mL.

The total reduction capability of the CF showed promising results for its antioxidant activities implying that it can protect the tissues from oxidative stress. Our result showed an increase in the absorbance at 700 nm and is depicted in Table 9. The minimum inhibitory percentage was observed at 100 µg/mL concentration is 0.30%, and the maximum inhibitory concentration at 500 µg/mL is 0.90%. The IC_{50} value observed was 419.14 µg/mL. This result demonstrated the capacity of CF to prevent the ROS formation and reduce the possibilities of stone formation.

Table 9 Effect on different radical-scavenging activities of CF of *P. gangeticus*

Concentration (μg/mL)	Inhibition (%)							
	DPPH radical scavenging activity		Nitric oxide scavenging activity		Superoxide dismutase		Reducing power	
	CF	AA	CF	AA	CF	AA	CF	AA
100	37.66 ± 0.57^{e}	44.33 ± 1.15^{e}	18.33 ± 0.57^{e}	26.33 ± 0.57^{e}	14.66 ± 0.57^{e}	16.33 ± 0.57^{e}	0.30 ± 0.05^{e}	0.32 ± 0.05^{e}
200	43.33 ± 1.15^{d}	55.33 ± 1.15^{d}	23.33 ± 1.15^{d}	31.33 ± 0.57^{d}	27.33 ± 1.15^{d}	29.33 ± 0.57^{d}	0.47 ± 0.01^{d}	0.58 ± 0.01^{d}
300	52.66 ± 0.57^{c}	65.33 ± 0.57^{c}	35.66 ± 0.57^{c}	39.33 ± 0.57^{c}	36.66 ± 0.57^{c}	38.66 ± 0.57^{c}	0.63 ± 0.05^{c}	0.69 ± 0.06^{e}
400	62.33 ± 0.57^{b}	77.33 ± 0.57^{b}	42.33 ± 0.57^{b}	47.00 ± 1.73^{b}	45.33 ± 0.57^{b}	47.33 ± 0.57^{b}	0.73 ± 0.05^{b}	0.78 ± 0.3^{d}
500	71.33 ± 0.57^{a}	83.66 ± 0.57^{a}	52.66 ± 0.57^{a}	61.66 ± 0.57^{a}	56.66 ± 0.57^{a}	59.66 ± 0.57^{a}	0.90 ± 0.04^{a}	1.18 ± 0.27^{b}
IC_{50} values	415.9327	334.4818	391.729	338.341	275.971	190.1591	419.14	310.1443

Values are mean of triplicate determination ($n = 3$) ± standard deviation; means bearing different superscripts (a/b/c/d/e) indicates significant difference when compared with control; $p < 0.05$; *CF*, chloroform fraction; *AA*, ascorbic acid

Table 10 Antibacterial activity of CF of *P. gangeticus*

Organism	Zone of inhibition (mm)		
	CF	Ampicillin	DMSO
Escherichia coli	11.00 ± 2.00	16.06 ± 1.10	00.00 ± 0.00
Staphylococcus aureus	8.46 ± 0.27	14.60 ± 0.57	00.00 ± 0.00
Klebsiella pneumoniae	12.33 ± 1.05	18.00 ± 1.00	00.00 ± 0.00

Data are presented in mean values ($n = 3$) ± standard deviation

Urolithiasis has a strong connection with the bacterial infections. Patients suffering from urolithiasis may have higher chances of urinary tract infections (UTI), and in some cases, the UTI may lead to the formation of kidney stones [90]. The term "infection stones" refer to the subset of urinary stones that consist of stone components associated with the UTIs [91]. Uropathogens such as *Escherichia coli*, *Staphylococcus aureus*, and *Pseudomonas aeruginosa* lead to the formation of UTIs and may cause the formation of kidney stones. The result of the antibacterial assay is depicted in Table 10. The maximum activity was observed in *Klebsiella pneumoniae* with a zone of inhibition (ZOI) of 12.33 ± 1.05 mm, and the minimum activity was observed in *Staphylococcus aureus* with a ZOI of 8.46 ± 0.27 mm. Our results suggest strong antibacterial potential of the CF against the selected uropathogens, also preventing UTI and stone formation. Several reports suggest the promising antibacterial potential of plants against uropathogens [92, 93].

Conclusion

P. gangeticus is an important medicinal plant having various pharmacological properties. In the present study, the CF of *P. gangeticus* showed good inhibition against CaOx crystal formation through nucleation and aggregation. The HPTLC profiling of CF showed the presence of many polyvalent compounds, and FTIR profiling gave the idea about the functional groups and nature of these polyvalent compounds. Moreover, the GC/MS analysis indicated that CF contains many biologically important phyto-constituents. The stigmasterol was found to be a major compound in CF. In this context, ADME-PK property of this molecule was established. To support antiurolithiatic activity of CF, its antioxidant and antibacterial properties were investigated. This is the first record of antiurolithiatic potential of *P. gangeticus* along with the antioxidant and antibacterial activity. In our laboratory, bioassay-guided studies are undergoing, which may lead to the identification of new antiurolithiatic agents from this plant species.

Acknowledgements Prof. B. D. Ranjitha Kumari acknowledges University Grants Commission (UGC), Government of India, New Delhi, India, for UGC-BSR Faculty Fellowship. The authors also thank DST-Purse (Phase 2), DST-FIST, UGC-SAP support to Department of Botany, Bharathidasan University, Tiruchirappalli-24, Tamil Nadu, India.

Author Contribution PKM and TPA planned and designed the experiments. PKM performed the experiments and AT helped to perform the experiments. PKM prepared the manuscript.TSK and BDRK collaborated with the critical analyses of the manuscript. All authors read and approved the final manuscript.

Declarations

Ethics Approval This is an observational study. The Research Ethics Committee has confirmed that no ethical approval is required.

Consent to Participate Not applicable.

Consent for Publication Not applicable.

Competing Interests The authors declare no competing interests.

References

1. Butterweck, V., & Khan, S. R. (2009). Herbal medicines in the management of urolithiasis: Alternative or complementary. *Planta medica, 75*(10), 1095–1103. https://doi.org/10.1055/s-0029-1185719
2. Boim, M. A., Heilberg, I. P., & Schor, N. (2010). *Phyllanthus niruri* as a promising alternative treatment for nephrolithiasis. *International Brazilian Journal of Urology, 36*(6), 657–664. https://doi.org/10.1590/S1677-55382010000600002
3. Porena, M., Guiggi, P., Balestra, A., & Micheli, C. (2004). Pain killers and antibacterial therapy for kidney colic and stones. *Urologia internationalis, 72*(Suppl. 1), 34–39. https://doi.org/10.1159/000076589
4. Khan, S. R., & Thamilselvan, S. (2000). Nephrolithiasis: A consequence of renal epithelial cell exposure to oxalate and calcium oxalate crystals. *Molecular urology, 4*(4), 305–312.
5. Zhang, D., Li, S., Zhang, Z., Li, N., Yuan, X., Jia, Z., & Yang, J. (2021). Urinary stone composition analysis and clinical characterization of 1520 patients in central China. *Scientific Reports, 11*, 6467. https://doi.org/10.1038/s41598-021-85723-3
6. Finkielstein, V. A., & Goldfarb, D. S. (2006). Strategies for preventing calcium oxalate stones. *Canadian Medical Association Journal, 174*(10), 1407–1409. https://doi.org/10.1503/cmaj.051517
7. Kennedy, J. (2005). Herb and supplement use in the US adult population. *Clinical therapeutics, 27*(11), 1847–1858. https://doi.org/10.1016/j.clinthera.2005.11.004
8. Bahmani, M., Baharvand-Ahmadi, B., Tajeddini, P., Rafieian-Kopaei, M., & Naghdi, N. (2016). Identification of medicinal plants for the treatment of kidney and urinary stones. *Journal of renal injury prevention, 5*(3), 129. https://doi.org/10.15171/jrip.2016.27
9. Bawari, S., Sah, A. N., & Tewari, D. (2021). Excavating the antiurolithiatic potential of wild Himalayan cherry through *in vitro* and preclinical investigations. *South African Journal of Botany*. https://doi.org/10.1016/j.sajb.2021.01.020
10. Mosquera, D. M. G., Ortega,Y. H., Quero,P. C., Martínez,R. S., & Pieters, L. (2020). Antiurolithiatic activity of *Boldoa purpurascens* aqueous extract: An *in vitro* and *in vivo* study. *Journal of ethnopharmacology* 253, 112691. https://doi.org/10.1016/j.jep.2020.112691
11. Taskin, T., Dogan, M., Yilmaz, B. N., Senkardes, I. (2020). Phytochemical screening and evaluation of antioxidant, enzyme inhibition, anti-proliferative and calcium oxalate anti-crystallization activities of *Micromeria fruticosa* spp. brachycalyx and *Rhus coriaria*. *Biocatalysis and Agricultural Biotechnology*. 27, 101670. https://doi.org/10.1016/j.bcab.2020.101670
12. Dias, E. R., Freire Dias, Td. L. M., Alexandre-Moreira, M. S., & Branco, A. (2020). Flavonoid-rich fraction from *Pleroma pereirae* (Melastomataceae): Effects on calcium oxalate crystallization, antioxidant and antinociceptive activities. *European Journal of Integrative Medicine*. https://doi.org/10.1016/j.eujim.2020.101095
13. Prasobh, K. M., Anil, K. M., Senthil, T. K., & Kumari, B. D. R. (2020). A comprehensive review of the phytochemical and pharmacological properties of *Desmodium gangeticum* (L.) DC. *Journal of Advanced Scientific Research, 11*(4), 90–97.
14. Chopra, R. N., Nayar, S. L., Chopra, I. C.(1956). Glossary of Indian medicinal plants, *CSIR, New Delhi*. 94.
15. Nadkarni, K.M. (1976). Indian materia medica, Popular Prakashan, Bombay, India.
16. Kiritikar, K. R., Basu, B. D. (1975).Indian medicinal plants 3, Bishen Singh & Mahendra Pal Sing, Dehra Dun, India.

17. Vaghela, B. D., Patel, B. R., & Pandya, P. N. (2012). A comparative pharmacognostical profile of *Desmodium* gangeticum DC. and *Desmodium laxiflorum* DC. *Ayu, 33*, 552–526. https://doi.org/10.4103/0974-8520.110522
18. Yasmeen, N., Ellandala, R., Sujatha, K., & Veenavamshee, R. (2011). Evaluation of renal protective effects of Desmodium Gangeticum L. in streptozotocin–induced diabetic rats. *International Journal of Research in Pharmacy and Chemistry, 1*(2), 121–128.
19. Changdar, N., Ganjhu, R. K., Rijal, S., Kumar, A., Mallik, S. B., Nampoothiri, M., Shenoy, R. R., Sonawane, K. B., Rao, M. C., & Mudgal, J. (2019). Exploring the potential of *Desmodium gangeticum* (L.) DC. Extract against spatial memory deficit in rats. *Pharmacognosy Magazine, 15*(62), S78–S83.
20. Karthikeyan, K., Selvam, G. S., Srinivasan, R., Chandran, C., Kulothungan, S. (2012). *In vitro* antibacterial activity of *Desmodium gangeticum* (L) DG Asian Pacific. *Journal of Tropical Disease, 2*(1), S421–S424. 10. 1016/ S2222- 1808(12) 60195–9
21. Bisht, R., Bhattacharya, S., & Jaliwala, Y. A. (2014). COX and LOX inhibitory potential of *Abroma augusta* and *Desmodium gangeticum*. *The Journal of Phytopharmacology, 3*(3), 168–175.
22. Jahan, F. I., Hossain, M. S., Mamun, A. A., Hossain, M. T., Seraj, S., Chowdhury, A. R., Khatun, Z., Andhi, N. Z., Chowdhury, M. H., & Rahmatullah, M. (2010). An evaluation of antinociceptive effect of methanol extracts of *Desmodium gangeticum* (L.) DC. stems and *Benincasa hispida* (Thunb.) Cogn. leaves on acetic acid induced gastric pain in mice. *Advances in Natural and Applied Sciences, 4*(3), 365–369.
23. Govindarajan, R., Vijayakumar, M., Shirwaikar, A., Rawat, A. K., Mehrotra, S., & Pushpangadan, P. (2006). Antioxidant activity of *Desmodium gangeticum* and its phenolics in arthritic rats. *Acta pharmaceutica (Zagreb Croatia), 56*(4), 489–496.
24. Sankar, V., Pangayarselvi, B., Prathapan, A., & Raghu, K. G. (2013). Desmodium gangeticum (Linn) DC exhibits antihypertrophic effect in isoproterenol-induced cardiomyoblasts via amelioration of oxidative stress and mitochondrial alterations. *Journal of cardiovascular pharmacology, 61*(1), 23–34. https://doi.org/10.1097/FJC.0b013e3182756ad3
25. Prasad, M. V. V., Balakrishna, K., & Carey, M. W. (2005). Hepatoprotective activity of roots of *Desmodium gangeticum* (Linn) DC. *Asian journal of chemistry, 17*(4), 2847–2849.
26 Singh, N., Mishra, P. K., Kapil, A., Arya, K. R., Maurya, R., & Dube, A. (2005). Efficacy of *Desmodium gangeticum* extract and its fractions against experimental visceral leishmaniasis. *Journal of ethnopharmacology, 98*(1–2), 83–88. https://doi.org/10.1016/j.jep.2004.12.032
27. Kim, E.-Y., Hong, S., Kim, J.-H., Kim, M., Lee, Y., Sohn, Y., & Jung, H.-S. (2021). Effects of chloroform fraction of *Fritillariae thunbergii* Bulbus on atopic symptoms in a DNCB-induced atopic dermatitis-like skin lesion model and in vitro models. *Journal of Ethnopharmacology, 281*, 114453. https://doi.org/10.1016/j.jep.2021.114453
28. Zoete, V., Daina, A., Bovigny, C., & Michielin, O. (2016). Swiss Similarity: A web tool for low to ultra high throughput ligand-based virtual screening. *Journal of Chemical Information and Modeling, 56*, 1399–1404.
29. Daina, A., Michielin, O., & Zoete, V. (2017). SwissADME: A free web tool to evaluate pharmacokinetics, drug-likeness and medicinal chemistry friendliness of small molecules. *Scientific Reports, 7*, 427–517.
30. Lipinski, C. A., Lombardo, F., Dominy, B. W., & Feeney, P. J. (1997). Experimental and computational approaches to estimate solubility and permeability in drug discovery and development settings. *Advanced Drug Delivery Reviews, 23*, 3–25.
31. Ghose, A. K., Viswanadhan, V. N., & Wendoloski, J. J. (1999). A knowledge-based approach in designing combinatorial or medicinal chemistry libraries for drug discovery. 1. A qualitative and quantitative characterization of known drug databases. *Journal of combinatorial chemistry, 1*, 55–68.
32. Veber, D. F., Johnson, S. R., Cheng, H. Y., Smith, B. R., Ward, K. W., & Kopple, K. D. (2002). Molecular properties that influence the oral bioavailability of drug candidates. *Journal of Medicinal Chemistry, 45*, 2615–2623.
33. Cortes, C., & Vapnik, V. (1995). Machine learning. *Support vector networks, 20*, 273–297.
34. Hennequin, C., Lalane, V., Daudon, M., Lacour, B., & Drueke, T. (1993). A new approach to studying inhibitors of calcium oxalate crystal growth. *Urological Research, 21*(2), 101–108. https://doi.org/10.1007/BF01788827
35. Patel, P. K., Patel, M. A., Vyas, B. A., Shah, D. R., & Gandhi, T. R. (2012). Antiurolithiatic activity of saponin rich fraction from the fruits of *Solanum xanthocarpum* Schrad. & Wendl. (Solanaceae) against ethylene glycol induced urolithiasis in rats. *Journal of Ethnopharmacology., 144*, 160–170. https://doi.org/10.1016/j.jep.2012.08.043
36 Sasikala, V., RamuRadha, S., & Vijakumari, B. (2013). *In vitro* evaluation of *Rotula aaquatica* Lour. for antiurolithiatic activity. *Journal of Pharmacy Research, 6*(1), 378–82. https://doi.org/10.1016/j.jopr.2013.02.026

37. Saha, S., & Verma, R. J. (2015). Evaluation of hydro-alcoholic extract of *Dolichos biflorus* seeds on inhibition of calcium oxalate crystallization. *Journal of Herbal Medicine, 5*(21), 41–47. https://doi.org/10.1016/j.hermed.2014.11.001
38 Blois, M. S. (1958). Antioxidant determinations by the use of a stable free radical. *Nature, 181*, 1199–1200. https://doi.org/10.1038/1811199a0
39 Kumar, K. N. S., Saraswathy, A., Amerjothy, S., Susan, T., & Ravishankar, B. (2014). Total phenol content and *in vitro* antioxidant potential of *Helicanthus* elastica (Desr.) Danser-a less-explored Indian mango mistletoe. *Journal of Traditional and Complementary Medicine, 4*(4), 285–288. https://doi.org/10.4103/2225-4110.130950
40. Kaur, P., & Arora, S. (2011). Superoxide anion radical scavenging activity of *Cassia siamea* and *Cassia javanica*. *Medicinal Chemistry Research, 20*(1), 9–15. https://doi.org/10.1007/s00044-009-9274-9
41. Vinod, M., Singh, M., Pradhan, M., Iyer, S. K., & Tripathi, D. K. (2012). Phytochemical constituents and pharmacological activities of Betula alba Linn. A review. *International Journal of Pharmacy Research and Technology, 4*(2), 643–647.
42. Perez, C. (1990). Antibiotic assay by agar-well diffusion method. *Acta biologiae et medicinae experimentalis, 15*, 113–115.
43. da Silva, R. F., Carneiro, C. N., de Sousa, C. B. D. C., Gomez, F. J., Espino, M., Boiteux, J., Dias, F. D. S. (2022). Sustainable extraction bioactive compounds procedures in medicinal plants based on the principles of green analytical chemistry: A review. *Microchemical Journal*, 107184. https://doi.org/10.1016/j.microc.2022.107184
44 Mohan, P. K., Adarsh Krishna, T. P., Senthil Kumar, T., & RanjithaKumari, B. D. (2021). Pharmaco-chemical profiling of *Desmodium gangeticum* (L.) DC. with special reference to soil chemistry. *Future Journal of Pharmaceutical Sciences, 7*(1), 1–11. https://doi.org/10.1186/s43094-021-00356-7
45. Chang, C., Yang, M., Wen, H., & Chern, J. (2002). Estimation of total flavonoid content in propolis by two complementary colorimetric methods. *Journal of Food and Drug Analysis, 10*(3), 178–182. https://doi.org/10.38212/2224-6614.2748
46. Dias, A. L. B., de Aguiar, A. C., Rostagno, M. A. (2021). Extraction of natural products using supercritical fluids and pressurized liquids assisted by ultrasound: Current status and trends. *Ultrasonics Sonochemistry*. 105584. https://doi.org/10.1016/j.ultsonch.2021.105584
47. Truong, D. H., Nguyen, D. H., Ta, N. T. A., Bui, A. V., Do, T. H., Nguyen, H. C.(2019). Evaluation of the use of different solvents for phytochemical constituents, antioxidants, and *in vitro* anti-inflammatory activities of *Severinia buxifolia. Journal of Food Quality*. 1–9. https://doi.org/10.1155/2019/8178294
48. Ngo Van, T., Scarlett, C.,Bowyer, M.,Ngo, P., Vuong, Q. (2017). Impact of different extraction solvents on bioactive compounds and antioxidant capacity from the root of *Salacia chinensis* L.. *Journal of Food Quality*. 1-8. https://doi.org/10.1155/2017/9305047
49. Lefebvre, T., Destandau, E., Lesellier, E. (2021). Selective extraction of bioactive compounds from plants using recent extraction techniques: A review. *Journal of Chromatography A*. 1635, 461770. https://doi.org/10.1016/j.chroma.2020.461770
50 Altemimi, A., Lakhssassi, N., Baharlouei, A., Watson, D., & Lightfoot, D. (2017). Phytochemicals:extraction, isolation, and identification of bioactive compounds from plant extracts. *Plants, 6*(4), 42. https://doi.org/10.3390/plants6040042
51. Kritika, M., Deepak, K., & Suresh, K. (2015). Antiamnesic activity of extracts and fraction of *Desmodium gangeticum*. *Journal of Pharmaceutical Technology Research and Management, 3*(1), 67–77. https://doi.org/10.15415/jptrm.2015.31006
52. Kurian, G. A., Srivats, R. S. S., Gomathi, R., Shabi, M. M., & Paddikkala, J. (2010). Interpretation of inotropic effect exhibited by *Desmodium gangeticum* chloroform root extract through GSMS and atomic mass spectroscopy: Evaluation of its anti ischemia reperfusion property in isolated rat heart. *Asian Journal of Biochemistry, 5*, 23–32. https://doi.org/10.3923/ajb.2010.23.32
53. Mishra, P. K., Singh, N., Ahmad, G., Dube, A., & Maurya, R. (2005). Glycolipids and other constituents from *Desmodium gangeticum* with antileishmanial and immunomodulatory activities. *Bioorganic and medicinal chemistry letters, 15*(20), 4543–4546. https://doi.org/10.1016/j.bmcl.2005.07.020
54 Yadav, K., Agrawal, A., Pal, J. A., & Gupta, M. M. (2013). Novel anti-inflammatory phyto constituents from *Desmodium gangeticum*. *Natural product research, 27*(18), 1639–1645. https://doi.org/10.1080/14786419.2012.761620
55 Mahajan, K., Kumar, D., Kaushik, D., & Kumar, S. (2017). Psychopharmacological evaluation of alkaloidal fraction of *Desmodium gangeticum*. *Journal of Biologically Active Products from Nature, 7*(1), 34–38. https://doi.org/10.1080/22311866.2017.1278720

56. Shradhanjali, S. S., Mishra, B., Mukerjee, A.(2019). *Clerodendrum serratum* (L.) Moon leaf extract and its chloroform fraction attenuates acute and chronic arthritis in albino rats. *Biocatalysis and Agricultural Biotechnology*.22, 101399. https://doi.org/10.1016/j.bcab.2019.101399
57. Ikpefan, E. O., Ayinde, B. A., Omeje, E. O., Azhar, M., Ahsana, D. F., Shah, Z. A., Shaheen, F, Choudhary, M. I. (2021). Isolation and anti-cancer evaluation of two anti-proliferative constituents from the chloroform fraction of leaves of *Conyza Sumatrensis* (Retz.) E. H. Walker, Asteraceae, *Scientific African*.13, e00854. https://doi.org/10.1016/j.sciaf.2021.e00854
58. Gabriel, O. A., Jamshed, I., Shafi, U. K., Sumera, Z., Khalid, R., Chukwu, E. O., Opeolu, O. O., & Nisar-ur-Rahman. (2019). Antidiabetic activities of chloroform fraction of *Anthocleista vogelii* Planch root bark in rats with diet- and alloxan-induced obesity-diabetes. *Journal of Ethnopharmacology, 229*, 293–302. https://doi.org/10.1016/j.jep.2018.10.021
59. Senguttuvan, J., Subramaniam, P.(2016). HPTLC fingerprints of various secondary metabolites in the traditional medicinal herb *Hypochaeris radicata* L. *Journal of Botany*. 1–11. https://doi.org/10.1155/2016/5429625
60 Attimarad, M., Ahmed, K. K., Aldhubaib, B. E., & Harsha, S. (2011). High-performance thin layer chromatography: A powerful analytical technique in pharmaceutical drug discovery. *Pharmaceutical methods, 2*(2), 71–75. https://doi.org/10.4103/2229-4708.84436
61. Krishna, T. P. A., Ajeesh, T. P., Chithra, N., Deepa, P., Darsana, U., Sreelekha, K., Juliet, Sanis, Nair, S., Ravindran, R., Ajith, K. K. G., Ghosh, S. (2014). Acaricidal activity of petroleum ether extract of leaves of *Tetrastigma leucostaphylum* (Dennst.) Alston against Rhipicephalus (Boophilus) annulatus. *The Scientific World Journal*.715481. https://doi.org/10.1155/2014/715481
62. Krishna, T. P. A., Palayullaparambil, T., Krishna, A., Juliet, S., Renganathan, K., Raju, R., Athalathil, S., Ravindran, R., Chandrashekar, L., Nair, S., & Ghosh, S. (2016). Pharmaco-Chemical characterization and acaricidal activity of ethanolic extract of *Chassalia Curviflora* (Wall ex Kurz.) Thwaites. *Pharmacognosy Journal, 8*, 215–219. https://doi.org/10.5530/pj.2016.3.6
63. Schulz, H., & Baranska, M. (2007). Identification and quantification of valuable plant substances by IR and Raman spectroscopy. *Vibrational Spectroscopy, 43*(1), 13–25. https://doi.org/10.1016/j.vibspec.2006.06.001
64. Younis, U., Rahi, A. A., Danish, S., Ali, M. A., Ahmed, N., Datta, R., & Glick, B. R. (2021). Fourier transform infrared spectroscopy vibrational bands study of *Spinacia oleracea* and *Trigonella corniculata* under biochar amendment in naturally contaminated soil. *PLoS One, 16*(6), e0253390. https://doi.org/10.1371/journal.pone.0253390
65 Gade, S., Rajamanikyam, M., Vadlapudi, V., Nukala, K. M., Aluvala, R., Giddigari, C., & Upadhyayula, S. M. (1861). (2017) Acetylcholinesterase inhibitory activity of stigmasterol & hexacosanol is responsible for larvicidal and repellent properties of *Chromolaena odorata*. *Biochimica et Biophysica Acta (BBA)-General Subjects, 1861*(3), 541–550. https://doi.org/10.1016/j.bbagen.2016.11.044
66. Alawode, T. T., Lajide, L., Olaleye, M., & Owolabi, B. (2021). Stigmasterol and β-sitosterol: Antimicrobial compounds in the leaves of *Lcacina trichantha* identified by GC–MS. *Beni-Suef University Journal of Basic and Applied Sciences, 10*(1), 1–8. https://doi.org/10.1186/s43088-021-00170-3
67. Gabay, O., Sanchez, C., Salvat, C., Chevy, F., Breton, M., Nourissat, G., & Berenbaum, F. (2010). Stigmasterol: A phytosterol with potential anti-osteoarthritic properties. *Osteoarthritis and cartilage, 18*(1), 106–116. https://doi.org/10.1016/j.joca.2009.08.019
68. Mahfuz, A., Salam, F. B. A., Deepa, K. N., & Hasan, A. N. (2019). Characterization of *in-vitro* antioxidant, cytotoxic, thrombolytic and membrane stabilizing potential of different extracts of *Cheilanthes tenuifolia* and stigmasterol isolation from n-hexane extract. *Clinical Phytoscience, 5*(1), 1–10. https://doi.org/10.1186/s40816-019-0135-x
69. Kaur, N., Chaudhary, J., Jain, A., & Kishore, L. (2011). Stigmasterol: A comprehensive review. *International Journal of Pharmaceutical Sciences and Research, 2*(9), 2259.
70. Eddershaw, P. J., Beresford, A. P., & Bayliss, M. K. (2000). ADME/PK as part of a rational approach to drug discovery. *Drug Discovery Today, 5*, 409–414.
71. Adarsh Krishna, T. P., Pandaram, S., & Ilangovan, A. (2019). Iron-mediated site-selective oxidative C-H/C–H cross-coupling of aryl radicals with quinones: Synthesis of β-secretase-1 inhibitor B and related arylated quinones. *Organic Chemistry Frontiers, 6*(18), 3244–3251. https://doi.org/10.1039/C9QO00623K
72. Adarsh Krishna, T. P., Pandaram, S., Chinnasamy, S., & Ilangovan, A. (2020). Oxidative radical coupling of hydroquinones and thiols using chromic acid: One-pot synthesis of quinonyl alkyl/aryl thioethers. *RSC Advances, 10*(33), 19454–19462. https://doi.org/10.1039/D0RA01519A
73. Krishna, T. A., Edachery, B., & Athalathil, S. (2022). Bakuchiol–a natural meroterpenoid: Structure, isolation, synthesis and functionalization approaches. *RSC advances, 12*(14), 8815–8832.
74. Abdel-Aal, E. A., Daosukho, S., & El-Shall, H. (2009). Effect of supersaturation ratio and Khella extract on nucleation and morphology of kidney stones. *Journal of crystal growth, 311*(9), 2673–2681. https://doi.org/10.1016/j.jcrysgro.2009.02.027

75. Coll, D. M., Varanelli, M. J., & Smith, R. C. (2002). Relationship of spontaneous passage of ureteral calculi to stone size and location as revealed by unenhanced helical CT. *American Journal of Roentgenology, 178*, 101–103. https://doi.org/10.2214/ajr.178.1.1780101
76. Sheng, X., Ward, M. D., & Wesson, J. A. (2005). Crystal surface adhesion explains the pathological activity of calcium oxalate hydrates in kidney stone formation. *Journal of the American Society of Nephrology, 16*(7), 1904–1908. https://doi.org/10.1681/ASN.2005040400
77. Hirayama, H., Wang, Z., Nishi, K., Ogawa, A., Ishimatu, T., Ueda, S., & Nohara, T. (1993). Effect of *Desmodium styracifolium*-triterpenoidon calcium oxalate renal stones. *British journal of urology, 71*(2), 143–147. https://doi.org/10.1111/j.1464-410X.1993.tb15906.x
78. Nirala, R. K., Dutta, P., Malik, M. Z., Dwivedi, L., Shrivastav, T. G., & Thakur, S. C. (2019). *In vitro* and *in silico* evaluation of betulin on calcium oxalate crystal formation. *Journal of the American College of Nutrition, 38*(7), 586–596. https://doi.org/10.1080/07315724.2019.1568321
79. Wesson, J. A., Worcester, E. M., Wiessner, J. H., Mandel, N. S., & Kleinman, J. G. (1998). Control of calcium oxalate crystal structure and cell adherence by urinary macromolecules. *Kidney International, 53*(4), 952–957. https://doi.org/10.1111/j.1523-1755.1998.00839.x
80. Atmani, F., & Khan, S. R. (2000). Effects of an extract from *Herniaria hirsuta* on calcium oxalate crystallization *in vitro*. *Bju International, 85*(6), 621–625.
81. Saha, S., & Verma, R. J. (2013). Inhibition of calcium oxalate crystallization *in vitro* by an extract of *Bergenia ciliata*. *Arab Journal of Urology, 11*(2), 187–192. https://doi.org/10.1016/j.aju.2013.04.001
82. YousefiGhale-Salimi, M., Eidi, M., Ghaemi, N., & Khavari-Nejad, R. A. (2018). Inhibitory effects of taraxasterol and aqueous extract of *Taraxacum officinale* on calcium oxalate crystallization: *in vitro* study. *Renal failure, 40*(1), 298–305. https://doi.org/10.1080/0886022X.2018.1455595
83. Aggarwal, K. P., Narula, S., Kakkar, M., & Tandon, C. (2013). Nephrolithiasis: Molecular mechanism of renal stone formation and the critical role played by modulators. *BioMed research international*. https://doi.org/10.1155/2013/292953
84. Barros, M. E., Schor, N., & Boim, M. A. (2003). Effects of an aqueous extract from *Phyllanthus niruri* on calcium oxalate crystallization *in vitro*. *Urological research, 30*, 374–379. https://doi.org/10.1007/s00240-002-0285
85. Perez, R. M. G., Vargas, R. S., Perez, S. G., Zavala, M. S., & Perez, C. G. (2000). Antiurolithiatic activity of 7-hydroxy-2′,4′,5′-trimethoxyisoflavone and 7-hydroxy-4′-methoxyisoflavone from *Eysenhardtia polystachya*. *Journal of Herbs Spices and Medicinal Plants, 7*(2), 27–34. https://doi.org/10.1300/J044v07n02_03
86. Khan, S. R. (2014). Reactive oxygen species, inflammation and calcium oxalate nephrolithiasis. *Translational andrology and urology, 3*(3), 256. https://doi.org/10.3978/j.issn.2223-4683.2014.06.04
87. Jyothilakshmi, V., Thellamudhu, G., Chinta, R., Alok, K., Anil, K., Debadatta, N., & Kalaiselvi, P. (2014). Beneficial antioxidative effect of the homeopathic preparation of *Berberis vulgaris* in alleviating oxidative stress in experimental urolithiasis. *Complementary Medicine Research, 21*(1), 7–12. https://doi.org/10.1159/000360240
88 Devkar, A. R., Chaudhary, S., Adepu, S., Xavier, S. K., Chandrashekar, K. S., & Setty, M. M. (2016). Evaluation of antiurolithiatic and antioxidant potential of *Lepidagathis prostrata*: A Pashanbhed plant. *Pharmaceutical Biology, 54*(7), 1237–1245. https://doi.org/10.3109/13880209.2015.1066397
89. Vermeulen, C.W. (1962). Experiments on causation of urinary calculi. Essays in experimental biology. *Chicago: University of Chicago Press*. 253–269.
90. Chen, D., Zhang, Y., Huang, J., Liang, X., Zeng, T., Lan, C., & Wu, W. (2018). The analysis of microbial spectrum and antibiotic resistance of uropathogens isolated from patients with urinary stones. *International journal of clinical practice, 72*(6), e13205. https://doi.org/10.1111/ijcp.13205
91. Bichler, K. H., et al. (2002). Urinary infection stones. *International Journal of Antimicrobial Agents, 19*, 488–498. https://doi.org/10.1016/S0924-8579(02)00088-2
92. Baloyi, I. T., Cosa, S., Combrinck, S., Leonard, C. M., & Viljoen, A. M. (2019). Anti-quorum sensing and antimicrobial activities of South African medicinal plants against uropathogens. *South African Journal of Botany, 122*, 484–491. https://doi.org/10.1016/j.sajb.2019.01.010
93. Bhandari, S., Khadayat, K., Poudel, S., Shrestha, S., Shrestha, R., Devkota, P., & Marasini, B. P. (2021). Phytochemical analysis of medicinal plants of Nepal and their antibacterial and antibiofilm activities against uropathogenic *Escherichia coli*. *BMC Complementary Medicine and Therapies, 21*(1), 1–11. https://doi.org/10.1186/s12906-021-03293-3

Authors and Affiliations

Prasobh K. Mohan[1] · T. P. Adarsh Krishna[2] · A. Thirumurugan[1] · T. Senthil Kumar[1] · B. D. Ranjitha Kumari[1]

[1] Department of Botany, Bharathidasan University, Tamil Nadu, Tiruchirappalli 620 024, India

[2] Research & Development Division, Sreedhareeyam Farmherbs India Pvt. Ltd, Ernakulam, Kerala 686-662, India